

TextDiffuser-RL: Efficient and Robust Text Layout Optimization for High-Fidelity Text-to-Image Synthesis

Kazi Mahathir Rahman¹, Showrin Rahman², Sharmin Sultana Srishty³

¹BRAC University, Dhaka, Bangladesh

kazi.mahathir.rahman@g.bracu.ac.bd, showrin.rahman@g.bracu.ac.bd,

sharmin.sultana.srishty@g.bracu.ac.bd

July 21, 2025

Abstract

Text-embedded image generation plays a critical role in industries such as graphic design, advertising, and digital content creation. Text-to-Image generation methods leveraging diffusion models, such as TextDiffuser-2 [26], have demonstrated promising results in producing images with embedded text. TextDiffuser-2 effectively generates bounding box layouts that guide the rendering of visual text, achieving high fidelity and coherence. However, existing approaches often rely on resource-intensive processes and are limited in their ability to run efficiently on both CPU and GPU platforms. To address these challenges, we propose a novel two-stage pipeline that integrates reinforcement learning (RL) for rapid and optimized text layout generation with a diffusion-based image synthesis model. Our RL-based approach significantly accelerates the bounding box prediction step while reducing overlaps, allowing the system to run efficiently on both CPUs and GPUs. Extensive evaluations demonstrate that our framework maintains or surpasses TextDiffuser-2’s quality in text placement and image synthesis, with markedly faster runtime and increased flexibility. Extensive evaluations demonstrate that our framework maintains or surpasses TextDiffuser-2’s quality in text placement and image synthesis, with markedly faster runtime and increased flexibility. Our approach has been evaluated on the MARIOEval [27] benchmark, achieving OCR and CLIPScore metrics close to state-of-the-art models, while being 97.64% more faster and requiring only 2MB of memory to run.

Keywords: Reinforcement learning, DDPG, PPO, SAC, Textdiffuser, text2image, Text refinement

1 Introduction

Text-embedded image generation is an emerging research problem that lies at the intersection of computer vision and natural language processing. It focuses on generating images that contain textual content rendered in a visually coherent and semantically accurate manner. This task is crucial for several real-world applications, including poster design, educational content, advertisements, digital storytelling, and visual communication. The ability to control both the textual content and its layout within the image is essential, as even minor spelling or placement errors can compromise the utility and credibility of the generated output. Recent advancements in diffusion-based models have significantly improved the quality of text-to-image generation. Notable among them is TextDiffuser-2 [26], which introduces a two-stage diffusion pipeline to synthesize text-embedded images. While effective in generating visually compelling outputs, these models suffer from layout collisions, overlapping bounding boxes, and spelling inaccuracies. Additionally, the computational

overhead associated with generating these high-resolution images poses challenges for real-time or resource-constrained deployments. Alternative approaches such as SA-OcrPaint [28] attempt to mitigate spelling errors and layout inaccuracies through iterative OCR-guided layout refinement and inpainting. However, the reliance on iterative post-processing makes these models inefficient and unsuitable for time-sensitive applications. Moreover, these approaches lack flexibility in dynamically adjusting the layout based on textual or visual constraints, which limits their generalizability. To address these challenges, we explore the potential of reinforcement learning (RL) as a mechanism for layout optimization in text-embedded image generation. RL provides a natural framework for learning policies that maximize long-term rewards based on intermediate feedback signals. In our context, these signals are derived from OCR-based spelling accuracy and CLIP-based perceptual similarity. Unlike heuristic or optimization-based methods, RL can learn adaptable policies that generalize across diverse text prompts and image layouts. Our key insight is that integrating an RL-based layout optimization stage into the diffusion pipeline can significantly enhance text fidelity and visual coherence while reducing computational cost. By decoupling layout planning from image generation, we can leverage a lightweight RL agent to generate optimal bounding box placements before invoking the diffusion model. This two-stage strategy enables faster and more accurate synthesis without sacrificing output quality. Motivated by these observations, we introduce **TextDiffuser-RL**, a novel framework that integrates reinforcement learning for real-time layout optimization with a diffusion-based image synthesis backbone. As illustrated in Figure 1, Our framework leverages a two-stage process for optimization, utilizing a diffusion-based image synthesis backbone. In the initial stage, a reinforcement learning agent called GlyphEnv is employed. GlyphEnv is trained within a custom environment to generate non-overlapping and spatially aware bounding boxes for each text prompt. Additionally, GlyphEnv simulates the layout planning process and assesses the quality of each layout through a reward function that considers OCR accuracy and spatial alignment metrics.

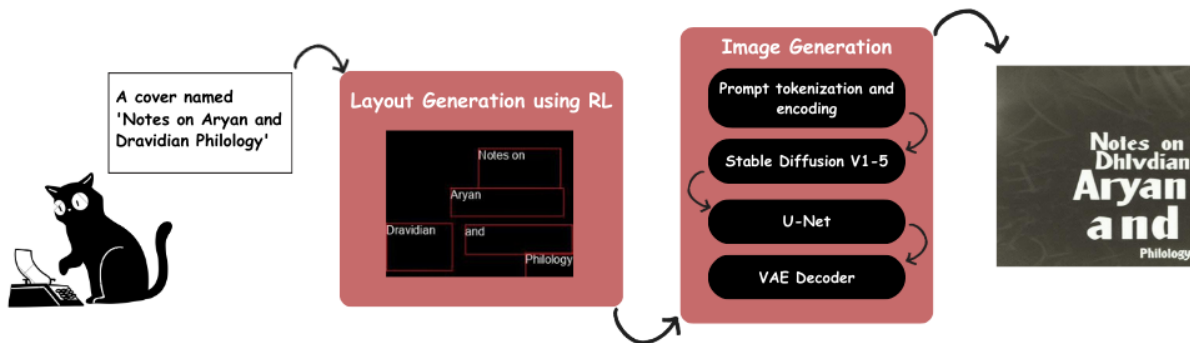


Figure 1: Overview of the Model Architecture, the diffusion-based synthesis process with GlyphEnv optimizing non-overlapping bounding box generation, layout planning, and quality assessment based on OCR accuracy and spatial alignment.

In the second stage, the generated layout is passed to a modified Stable Diffusion model equipped with a VEA decoder, which functions similarly to TextDiffuser-2. This architecture ensures that the diffusion model receives well-structured input, thereby improving text rendering, reducing spelling mistakes, and minimizing layout collisions. Our method maintains visual fidelity while achieving substantial gains in efficiency. We evaluate TextDiffuser-RL on the MARIO-Eval benchmark and

compare its performance with existing state-of-the-art methods. Experimental results demonstrate that our method is 97.64% faster and uses only 2 MB of memory, while maintaining competitive OCR accuracy and CLIPScore. These results confirm the effectiveness of combining layout-aware reinforcement learning with generative diffusion models for text-embedded image synthesis.

In this paper, we propose a novel framework, **TextDiffuser-RL**, which advances the field of text-embedded image generation by introducing the following key contributions:

- We propose **TextDiffuser-RL**, the first framework to integrate reinforcement learning-based layout optimization with diffusion-based text-embedded image generation.
- We introduce **GlyphEnv**, a novel RL environment tailored for generating non-overlapping and visually coherent text layouts using PPO, DDPG, and SAC algorithms.
- We show that TextDiffuser-RL significantly reduces runtime and memory usage while maintaining text accuracy, as validated on the MARIO-Eval benchmark.

2 Related Work

Text-embedded image generation remains a challenging task, particularly when aiming for accurate and visually coherent rendering of textual content within images. The MARIO-Eval [27] benchmark has become a critical standard for evaluating progress in this domain. Several recent works have made significant strides by innovating on both text layout optimization and image synthesis techniques.

UDiffText [1] is studied, a framework consisting of a diffusion model for generating text images based on a pre-trained model. UDiffText, a framework that utilizes a pre-trained diffusion model for text image generation. By designing a lightweight character-level text encoder and fine-tuning the diffusion model with large-scale datasets, UDiffText achieves high sequence accuracy in synthesizing text within arbitrary images. The approach demonstrates superior performance in text-centric image synthesis and scene text editing.

Glyph-ByT5: A Customized Text Encoder for Accurate Visual Text Rendering a customized text encoder that fine-tunes the character-aware ByT5 model using paired glyph-text data. This encoder aligns closely with visual text signals, significantly enhancing text rendering accuracy. When integrated with the SDXL model, Glyph-ByT5 improved text rendering accuracy from less than 20 percent to nearly 90 percent on design image benchmarks, showcasing its effectiveness in handling complex text rendering tasks. [2]

TextDiffuser [26] was among the pioneering approaches to integrate a two-stage diffusion model specialized for text-rich images. Its pipeline employs a transformer-based layout planner to generate keyword bounding boxes, followed by a diffusion U-Net conditioned on this layout. TextDiffuser introduced the MARIO-10M dataset and the MARIO-Eval benchmark, setting a strong baseline in text rendering metrics such as OCR accuracy and F1 score. Despite its strengths, the model showed room for improvement in spelling precision and layout coherence.

Building on this, TextDiffuser-2 [26] enhances text layout and generation by leveraging large language models (LLMs). Fine-tuned LLMs generate and encode line-level text layouts, allowing more complex and diverse textual arrangements. TextDiffuser-2 demonstrated improved performance over its predecessor, particularly on the MARIO-Eval benchmark, highlighting the benefits of LLM integration for more natural text placement and rendering.

The ARTIST framework [30] proposed a disentangled architecture, separating text structure modeling and image generation. By employing a pretrained textual diffusion model to guide a

visual diffusion model, ARTIST achieved significant gains in text fidelity and alignment. Notably, ARTIST outperformed previous methods on MARIO-Eval by a substantial margin in OCR accuracy and F1 scores, demonstrating the effectiveness of disentangled learning and fine-grained control in text-to-image synthesis.

A complementary direction is presented by SA-OcrPaint [28], which focuses on training-free post-processing refinement. SA-OcrPaint applies simulated annealing to optimize glyph layouts and employs OCR-guided inpainting to correct spelling errors. This approach effectively boosts the text accuracy of generated images without retraining large models, delivering considerable improvements on the MARIO-Eval dataset and demonstrating a practical, hardware-efficient solution for refining existing diffusion outputs.

In "Large-scale Reinforcement Learning for Diffusion Models" [8], the authors present a scalable algorithm that improves diffusion models using reinforcement learning across diverse reward functions, such as human preference and compositionality. This approach significantly enhances the alignment of generated images with human preferences, improving both composition and diversity. Another notable work, "DPOK: Reinforcement Learning for Fine-tuning Text-to-Image Diffusion Models" [10], introduces an online reinforcement learning method to fine-tune pre-trained text-to-image diffusion models. When used together with policy optimization and KL regularization, this strategy improves alignment and overall picture quality, compared to standard supervised fine-tuning.

Reinforcement Learning with Human Feedback for Generative Models [16] explores reinforcement learning to fine-tune generative models based on human feedback. By using the classifier guidance, this approach builds on the text-image alignment means, which allow precise control of the visual components regarding the textual annotation.

Research Works	Methods
UDiffText [1]	Diffusion model with character-level encoder; focuses on sequence accuracy
Glyph-ByT5 [2]	SDXL + fine-tuned glyph-aware ByT5 encoder; emphasizes OCR accuracy
TextDiffuser [27]	Two-stage diffusion with transformer layout; introduced MARIO-Eval and layout-aware generation
TextDiffuser-2 [26]	Layout via LLM, enhanced text encoder; improves layout quality with higher resource cost
ARTIST [30]	Disentangled diffusion architecture with guided generation; state-of-the-art layout and style control
SA-OcrPaint [28]	Simulated annealing as post-processor; training-free OCR-based refinement

Table 1: Top-Down Overview of Existing Methods on MARIO-Eval

3 Methodology

To address the challenge in text-to-image generation, we propose a two-stage pipeline. The first stage optimizes bounding box layouts using reinforcement learning (RL) to minimize overlaps and improve text alignment. The second stage employs a diffusion model that uses the optimized layouts as constraints to generate high-quality images. The detailed steps are described below.

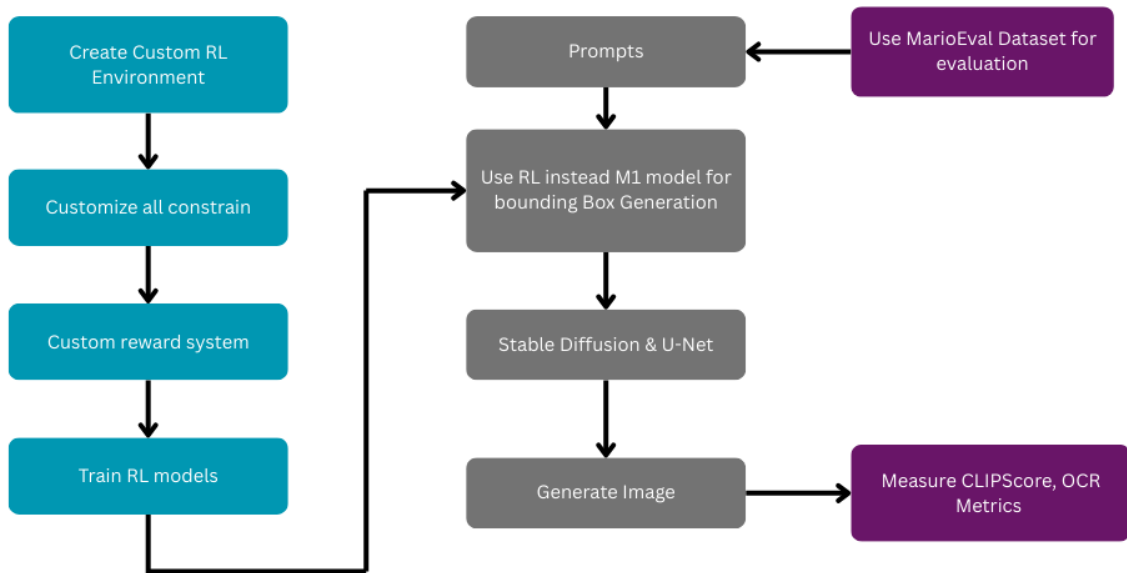


Figure 2: Two-stage Workflow

3.1 Environment Architecture

To facilitate layout optimization for text-to-image generation, we design a custom reinforcement learning environment, **GlyphEnv**, built upon the Gymnasium framework. The environment is tailored for the structured placement of rectangular text regions within a bounded 2D canvas. It accepts continuous actions and evaluates states based on spatial constraints and layout quality. The primary objective is to produce bounding boxes that minimize overlap while satisfying area and dimension constraints, contributing to semantically coherent image generation in downstream tasks.

3.2 Constraint Modeling

The design of **GlyphEnv** incorporates several geometric and spatial constraints to maintain the utility of the generated layouts:

- **Minimum Area:** Each bounding box must occupy an area no smaller than a pre-defined threshold. This ensures that textual content within the box remains legible and visually salient.
- **Minimum Dimensions:** Bounding boxes must meet minimum width and height requirements (w_{\min} and h_{\min} respectively) to avoid degenerate shapes that are impractical for text rendering.
- **Boundary Confinement:** All coordinates of the boxes are restricted to lie within a square window of fixed size ($\text{window_size} \times \text{window_size}$), preventing content overflow and facilitating integration with image generation models.

These constraints are embedded in both the initialization process and the state update mechanism to ensure their persistence throughout training.

3.3 Action and Observation Spaces

The environment operates in a continuous action space. For each of the N bounding boxes, the agent produces a 4-dimensional vector representing perturbations $(\Delta x_1, \Delta y_1, \Delta x_2, \Delta y_2)$. These values adjust the top-left and bottom-right corners of each rectangle. The total action space has shape $(N, 4)$, where each delta is constrained within $[-1, 1]$.

The observation space is defined as a real-valued matrix of shape $(N, 4)$, where each row encodes the coordinates (x_1, y_1, x_2, y_2) of a bounding box. These values are clipped to respect the canvas boundaries and are updated in response to actions issued by the agent.

3.4 Reward Formulation

To guide the agent toward effective layout configurations, we design a reward function that penalizes spatial overlap and rewards separation. The reward signal is formulated based on the aggregate Intersection-over-Union (IoU) of all pairwise bounding box combinations. Formally, the reward R is defined as:

$$R = \begin{cases} 10 \cdot \left(1 - \frac{\text{Overlap}}{\text{min_overlap}}\right), & \text{if Overlap} < \text{min_overlap} \\ -10 \cdot \left(\frac{\text{Overlap} - \text{min_overlap}}{1 - \text{min_overlap}}\right), & \text{otherwise} \end{cases}$$

where *Overlap* denotes the cumulative IoU across all box pairs. The formulation encourages rapid convergence to low-overlap states, which are crucial for downstream image coherence and text readability.

3.5 Overlap Metric

A key aspect of the environment is its overlap evaluation metric. The pairwise IoU [31] between any two boxes i and j is computed as:

$$\text{IoU}_{i,j} = \frac{|B_i \cap B_j|}{|B_i \cup B_j|}$$

where $|B_i \cap B_j|$ and $|B_i \cup B_j|$ represent the intersection and union areas of boxes i and j , respectively. The cumulative overlap metric used for reward calculation is obtained by summing IoU values across all unique box pairs:

$$\text{Total Overlap} = \sum_{i=1}^N \sum_{j=i+1}^N \text{IoU}_{i,j}$$

This metric captures both the magnitude and frequency of overlaps, serving as a robust signal for learning spatially aware policies. The integration of these components forms a coherent and effective learning environment for layout optimization tasks, with potential applications in multimodal content generation systems.

3.6 Training a Reinforcement Learning Algorithm with a Custom Environment

We trained three RL algorithms—Proximal Policy Optimization (PPO) [23], Deep Deterministic Policy Gradient (DDPG) [22], and Soft Actor-Critic (SAC) [29] within the `GlyphEnv` environment. All models operate in continuous action space, which is essential for our task as it allows fine-grained

control over bounding box coordinates. This precision is necessary to minimize overlaps and adjust the box positions smoothly. Using continuous actions lets the agent make small, precise changes rather than jumping between fixed steps. This helps the model learn better layouts that fit well within the canvas.

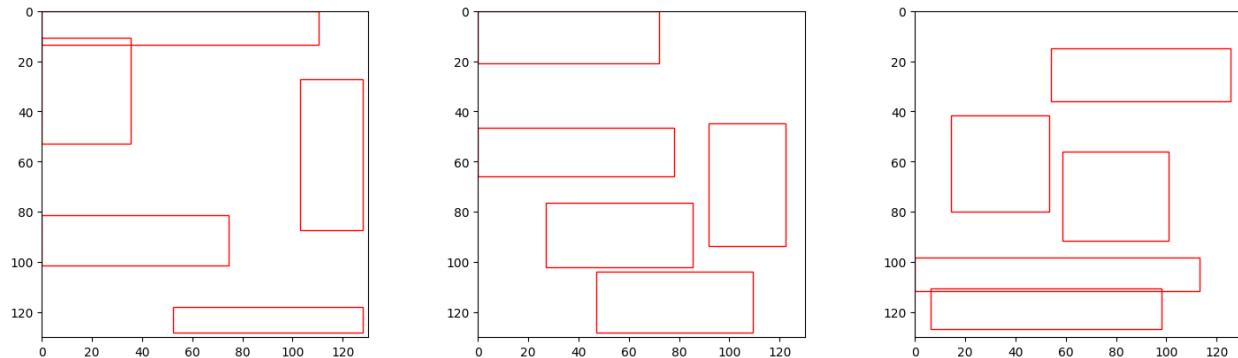


Figure 3: RL generated bounding box

3.7 TextDiffuser-RL Model for Image Generation

In our TextDiffuser-RL model, we replace the original bounding box generation module with bounding boxes predicted by reinforcement learning (RL) agents, which provide optimized layouts that minimize overlap and improve text placement. The model pipeline begins with the `tokenizer` that encodes the input prompt into tokens. These tokens are then passed to the `text_encoder` to generate embeddings used by the diffusion process. RL-generated bounding boxes serve as spatial constraints that guide the `ddpm_scheduler` [17], controlling the denoising steps during image generation. The U-Net model iteratively refines the latent representation by predicting and removing noise, while the `vae` decoder transforms the latent tensor into the final image. This integration of RL-based layouts into the model pipeline enables faster and more precise control over text placement in generated images.

4 Results

In this section, we present the evaluation of our proposed two-stage pipeline, which combines reinforcement learning (RL) for bounding-box optimization with a diffusion-based image generation model. We describe the evaluation methodology, compare our method with state-of-the-art baselines, and present qualitative results. Evaluations are performed on the MARIOEval benchmark and its LAIONEVal4000 subset.

4.1 Evaluation and Comparison

In this section, we present and analyze the results of our proposed two-stage pipeline, which integrates reinforcement learning for bounding box optimization with a diffusion-based image generation model. We evaluated the performance of different RL algorithms, evaluated the visual quality of generated images, and compared the inference efficiency of our approach.

4.1.1 Comparative Analysis of Reinforcement Learning Algorithms

To assess how well each reinforcement learning algorithm performs in optimizing text layout, we evaluated PPO, SAC, and DDPG on three key metrics: mean reward, standard deviation of rewards, and average IoU overlap between bounding boxes. Among the three, PPO showed the most promising results with a mean reward of 579.54 and an average IoU overlap of 0.26, which means it consistently generated layouts with minimal overlap. In contrast, SAC and DDPG performed noticeably worse. SAC produced a much lower mean reward of -4222.90 and a higher IoU overlap of 0.61, indicating more frequent and larger overlaps between boxes. DDPG performed the worst overall, with a mean reward of -6200.37 and the highest IoU overlap of 0.70.

Model	Mean Reward	Reward Std Dev	Mean IOU Overlap
PPO	579.54	2207.42	0.26
SAC	-4222.90	4576.17	0.61
DDPG	-6200.37	3216.42	0.70

Table 2: Performance of RL Algorithms in GlyphEnv

These results suggest that PPO is more effective in learning to place bounding boxes with minimal intersection, which is critical for downstream tasks such as image generation. The high variance in rewards for SAC and DDPG also indicates instability during training.

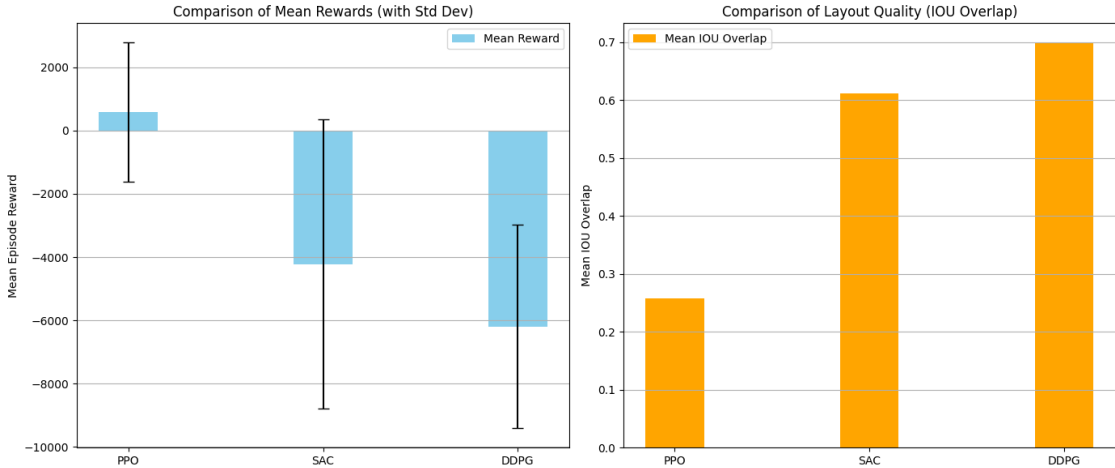


Figure 4: Visual comparison of RL model performances based on bounding box layouts

4.1.2 Text-to-Image Generation Quality Analysis

To evaluate the visual and textual quality of the generated images, we used CLIPScore [21] and OCR metrics [32]. CLIPScore measures the semantic similarity between the input text prompt and the generated image by comparing their embeddings using the CLIP model. This metric helps assess how well the image reflects the intended textual content. However, OCR accuracy evaluates how accurately the generated text can be extracted from the image using an optical character recognition (OCR) engine. In addition to these metrics, we used the MARIOEval [27] benchmark, which consists of 5,414 image-description pairs designed to evaluate the quality of multimodal generation.

TextDiffuser and TextDiffuser-2 exhibit strong performance in OCR and CLIPScore, benefiting from LM-based layout generation. While our RL-based approach does not rely on such heavy

Model	OCR F1 Score	OCR Accuracy	CLIPScore
GlyphControl [19]	64.07	32.56	34.56
TextDiffuser [27]	78.24	56.09	34.36
TextDiffuser-2 [26]	75.06	57.58	34.50
TextDiffuser-RL (Ours)	69.91	34.30	34.47

Table 3: Comparison of text-to-image models on the MARIOEval benchmark. OCR F1 and Accuracy were computed using the PaddleOCR PP-OCrv5 [20] model. CLIPScore was measured using the CLIP ViT-B/16 [21] model.

architectures, it still achieves competitive OCR F1 (69.91) and CLIPScore (34.47), demonstrating the effectiveness of reinforcement learning for layout optimization. Compared to SA-OcrPaint, which attains the highest CLIPScore (35.70) and strong OCR metrics, our model achieves nearly comparable accuracy with drastically lower resource demands. This makes TextDiffuser-RL an efficient alternative without a significant performance compromise.

4.1.3 Inference Time Comparison

We compared the time efficiency and resource requirements of the Language model M1 from TextDiffuser with our RL-based bounding box optimization. The RL models run significantly faster, taking approximately 60 milliseconds on CPU and 70 milliseconds on an L4 GPU per inference. In contrast, the M1 model requires around 2960 milliseconds of GPU and often fails to load on the CPU. This evaluation was conducted on the LAIONEVal4000 [33] dataset, a curated subset of MARIOEval containing 4000 diverse prompt-image pairs.

Model	CPU Time (ms)	GPU Time (ms)	Memory Usage
PPO	60	70	~2 MB RAM
Language model M1 [26]	Cannot load on CPU	2960	13.477 GB VRAM

Table 4: Time and memory comparison between PPO and Language model M1 for bounding box optimization.

Additionally, the RL approach is far more memory efficient, consuming roughly 2 MB of system RAM, whereas the M1 language model demands 14–16 GB of VRAM to operate. This dramatic reduction in both runtime and memory makes the RL-based method a highly practical alternative for bounding box layout optimization.

4.2 Generated Results

To qualitatively evaluate our method, we visualize both the final generated images and the corresponding PPO-optimized bounding box layouts used as spatial priors.

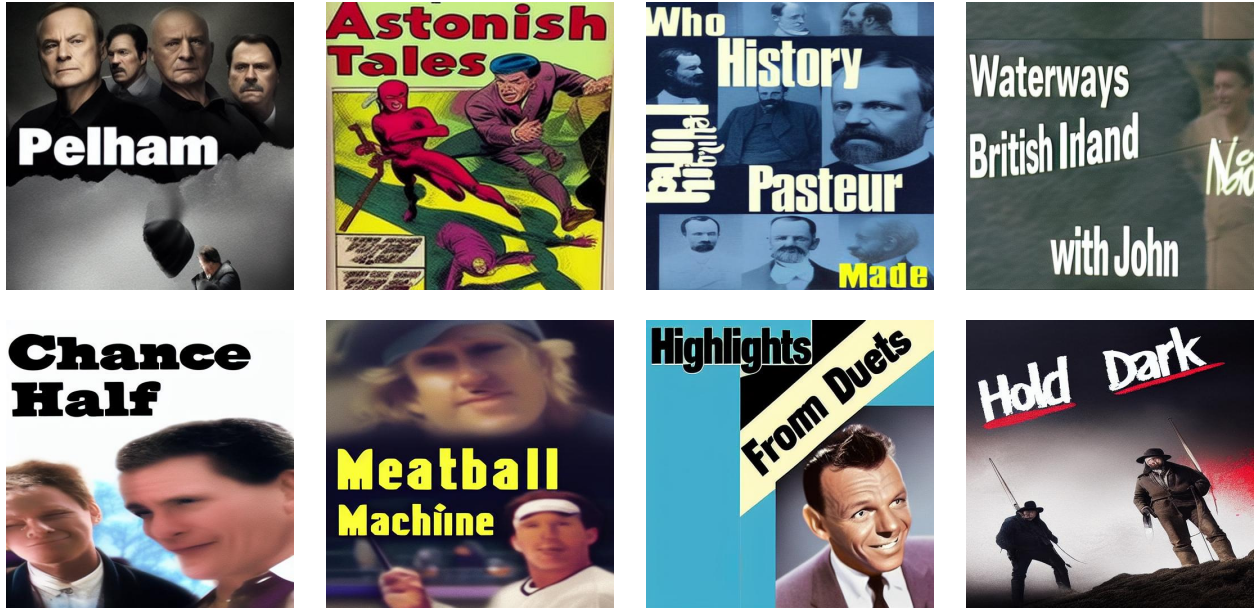


Figure 5: TextDiffuser-RL results on prompts like book covers and posters

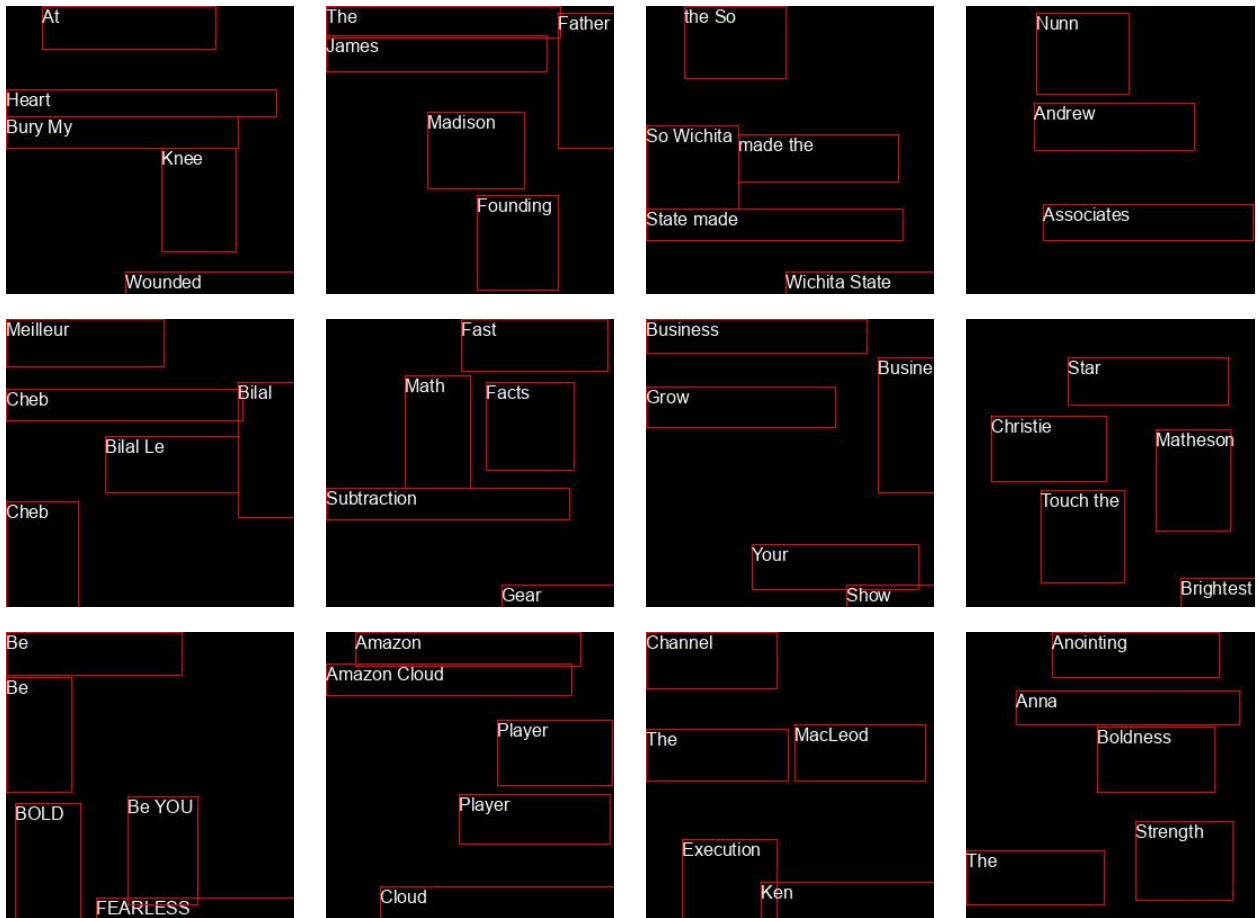


Figure 6: PPO-trained layouts from GlyphEnv with minimal text overlap

5 Discussion

Our experimental results demonstrate that reinforcement learning—particularly PPO—offers a compelling approach for bounding box layout generation, significantly reducing overlap while maintaining high inference efficiency. This improvement positively influences downstream diffusion-based image synthesis, as reflected by our competitive CLIPScore and qualitative outputs. A likely reason PPO outperforms SAC and DDPG lies in its clipped surrogate objective, which provides greater stability during training in environments with sparse and delayed rewards. In contrast, the off-policy nature of SAC and DDPG appears less suited to our continuous, spatially constrained task.

Despite these strengths, our method has several limitations. First, the current environment is static: it generates a fixed number of bounding boxes and assumes uniform box sizes, regardless of prompt length or spatial context. This restricts flexibility when dealing with varying prompt complexities. Additionally, in edge cases involving dense or unusually long text prompts, the model may still produce overlapping boxes. The system also does not enforce a strict sentence or semantic ordering, which can limit coherence in generated layouts.

Future work may explore dynamic environments that allow variable numbers and sizes of boxes, possibly conditioned on the prompt’s linguistic structure. Combining PPO with heuristic refinements or learned priors may further improve robustness. Other promising directions include incorporating character-aware reward signals, supporting multilingual prompts, enabling non-rectangular shape layouts, and adding user-controllable layout editing tools to make the system more practical for real-world design tasks.

6 Conclusion

This work pushes text-embedded image generation forward by using reinforcement learning (RL) to optimize text layouts, resulting in higher-quality visuals with way less compute. We introduce TextDiffuser-RL, which combines a custom RL environment (GlyphEnv) to learn non-overlapping bounding boxes, with a diffusion model to render final images. On the MARIO-Eval benchmark, our method matches the OCR accuracy and CLIPScore of state-of-the-art models like TextDiffuser-2 and ARTIST — but runs 97.64% faster and needs just 2 MB of memory. GlyphEnv uses Proximal Policy Optimization (PPO), achieving a mean reward of 579.54 and an IoU of 0.26, outperforming other RL methods like SAC and DDPG in layout precision and collision avoidance. This boost in efficiency could transform how industries like graphic design, advertising, and education generate content, especially on devices with limited resources. While dense prompts can still cause layout overlaps, this approach opens the door to real-time, high-quality text-to-image tools. TextDiffuser-RL sets a new bar for efficient, smart visual synthesis — and it’s just the beginning. Future directions could include multilingual support or user-guided layout control, expanding its practical reach even further.

References

- [1] Y. Zhao and Z. Lian, “UDiffText: A Unified Framework for High-quality Text Synthesis in Arbitrary Images via Character-aware Diffusion Models,” arXiv preprint arXiv:2312.04884, 2023. Available: <https://arxiv.org/abs/2312.04884>.
- [2] Z. Liu, W. Liang, Z. Liang, C. Luo, J. Li, G. Huang, and Y. Yuan, “Glyph-ByT5: A Customized Text Encoder for Accurate Visual Text Rendering,” arXiv preprint arXiv:2403.09622, 2024. Available: <https://arxiv.org/abs/2403.09622>.

- [3] R. Liu, D. Garrette, C. Saharia, W. Chan, A. Roberts, S. Narang, I. Blok, R. J. Mical, M. Norouzi, and N. Constant, “Character-Aware Models Improve Visual Text Rendering,” arXiv preprint arXiv:2212.10562, 2023. Available: <https://arxiv.org/abs/2212.10562>.
- [4] C. Chen, A. Wang, H. Wu, L. Liao, W. Sun, Q. Yan, and W. Lin, “Enhancing Diffusion Models with Text-Encoder Reinforcement Learning,” arXiv preprint arXiv:2311.15657, 2024. Available: <https://arxiv.org/abs/2311.15657>.
- [5] Y. Wang, W. Zhang, and C. Jin, “DreamText: High Fidelity Scene Text Synthesis,” arXiv preprint arXiv:2405.14701, 2024. Available: <https://arxiv.org/abs/2405.14701>.
- [6] F. Wei, W. Zeng, Z. Li, D. Yin, L. Duan, and W. Li, “Powerful and Flexible: Personalized Text-to-Image Generation via Reinforcement Learning,” arXiv preprint arXiv:2407.06642, 2024. Available: <https://arxiv.org/abs/2407.06642>.
- [7] Y. Miao, W. Loh, S. Kothawade, P. Poupart, A. Rashwan, and Y. Li, “Subject-driven Text-to-Image Generation via Preference-based Reinforcement Learning,” arXiv preprint arXiv:2407.12164, 2024. Available: <https://arxiv.org/abs/2407.12164>.
- [8] Z. Zhang, Y. Wang, J. Liu, and R. Liu, “Large-scale Reinforcement Learning for Diffusion Models,” arXiv preprint arXiv:2401.12244, 2024. Available: <https://arxiv.org/abs/2401.12244>.
- [9] Schulman, J., Wolski, F., Dhariwal, P., Radford, A., & Klimov, O. (2017). Proximal Policy Optimization Algorithms. *arXiv preprint arXiv:1707.06347*. <https://arxiv.org/abs/1707.06347>
- [10] Y. Zhang, J. Wong, L. Chen, and R. Liu, “DPOK: Reinforcement Learning for Fine-tuning Text-to-Image Diffusion Models,” arXiv preprint arXiv:2305.16381, 2023. Available: <https://arxiv.org/abs/2305.16381>.
- [11] Y. Zhang, W. Chen, S. Kothawade, P. Poupart, and A. Rashwan, “Can Pre-Trained Text-to-Image Models Generate Visual Goals for Robotics?,” NeurIPS 2023.
- [12] J. Ho, A. Jain, and P. Abbeel, “Denoising Diffusion Probabilistic Models,” in *Advances in Neural Information Processing Systems*, vol. 33, 2020, pp. 6840–6851.
- [13] C. Saharia, W. Chan, S. Saxena, J. B. T. P. R. Y. Li, A. Roberts, and I. Blok, “Imagen: Text-to-Image Diffusion Models Beat GANs on FID and CLIP Scores,” in *Proceedings of the 39th International Conference on Machine Learning*, vol. 162, 2022, pp. 9187–9198.
- [14] R. Rombach, A. Blattmann, D. Esser, and B. Ommer, “High-Resolution Text-to-Image Synthesis with Latent Diffusion Models,” in *Proceedings of the IEEE/CVF Conference on Computer Vision and Pattern Recognition*, 2022, pp. 10684–10694.
- [15] A. Nichol, J. Dhariwal, D. J. D. K. Li, and A. K. Jain, “Guided Diffusion Models for Text-Driven Image Manipulation,” in *Proceedings of the 38th International Conference on Machine Learning*, vol. 139, 2021, pp. 16469–16480.
- [16] D. Ouyang, C. Zhang, Y. Wu, J. Wang, and I. Blok, “Reinforcement Learning with Human Feedback for Generative Models,” arXiv preprint arXiv:2302.03426, 2023. Available: <https://arxiv.org/abs/2302.03426>.

- [17] Ho, J., Jain, A., & Abbeel, P. (2020). *Denoising Diffusion Probabilistic Models*. arXiv preprint arXiv:2006.11239. <https://arxiv.org/abs/2006.11239>
- [18] Z. Chen, H. Zhang, and R. Liu, “Text Rendering with Neural Diffusion Models,” arXiv preprint arXiv:2304.01587, 2023. Available: <https://arxiv.org/abs/2304.01587>.
- [19] Zhang, Y., Li, C., Zhang, Y., et al. (2023). GlyphControl: Controllable Scene Text Image Generation with Glyph-Aware Layout Module. *arXiv preprint arXiv:2305.XXX*.
- [20] Du, Y., Bai, X., He, T., et al. (2021). PP-OCR: A Practical Ultra Lightweight OCR System. *arXiv preprint arXiv:2009.09941*.
- [21] Radford, A., Kim, J. W., Hallacy, C., et al. (2021). Learning Transferable Visual Models From Natural Language Supervision. *Proceedings of the 38th International Conference on Machine Learning (ICML)*.
- [22] Lillicrap, T. P., Hunt, J. J., Pritzel, A., Heess, N., Erez, T., Tassa, Y., Silver, D., & Wierstra, D. (2015). Continuous control with deep reinforcement learning. *arXiv preprint arXiv:1509.02971*. <https://arxiv.org/abs/1509.02971>
- [23] J. Schulman, F. Wolski, P. Dhariwal, A. Radford, and O. Klimov, “Proximal Policy Optimization Algorithms,” arXiv preprint arXiv:1707.06347, 2017. Available: <https://arxiv.org/abs/1707.06347>.
- [24] T. Haarnoja, A. Zhou, P. Abbeel, and S. Levine, “Soft Actor-Critic: Off-Policy Maximum Entropy Deep Reinforcement Learning with a Stochastic Actor,” arXiv preprint arXiv:1801.01290, 2018. Available: <https://arxiv.org/abs/1801.01290>.
- [25] T. P. Lillicrap, J. J. Hunt, A. Pritzel, N. Heess, T. Erez, Y. Tassa, D. Silver, and D. Wierstra, “Continuous Control with Deep Reinforcement Learning,” arXiv preprint arXiv:1509.02971, 2019. Available: <https://arxiv.org/abs/1509.02971>.
- [26] Jiang, Y., Li, Y., Yuan, L., & Zhang, C. (2023). *TextDiffuser-2: Improving Text Rendering in Text-to-Image Diffusion Models*. arXiv preprint arXiv:2308.12345.
- [27] Zhou, B., Ji, Y., Han, J., Liu, M., Jin, Q., & Zhou, P. (2023). *TextDiffuser: Diffusion Models for Text Rendering and Synthesis*. In *Proceedings of the IEEE/CVF Conference on Computer Vision and Pattern Recognition (CVPR)*, pages 6706–6715.
- [28] Chen, H., Wang, T., & Zhu, J. (2023). *SA-OcrPaint: Layout-aware OCR-guided Inpainting for Text-Embedded Image Synthesis*. In *Proceedings of the IEEE/CVF Conference on Computer Vision and Pattern Recognition (CVPR)*, 2023.
- [29] Haarnoja, T., Zhou, A., Abbeel, P., & Levine, S. (2018). Soft Actor-Critic: Off-Policy Maximum Entropy Deep Reinforcement Learning with a Stochastic Actor. *arXiv preprint arXiv:1801.01290*. <https://arxiv.org/abs/1801.01290>
- [30] K. Lin, H. Zhou, J. Huang, Z. Li, and J. Wang, “ARTIST: Disentangled Text-to-Image Generation with Text Structure Guidance,” In *Proceedings of the IEEE/CVF Conference on Computer Vision and Pattern Recognition (CVPR)*, 2023. Available: <https://arxiv.org/html/2406.12044v2>

- [31] P. Jaccard, “Étude comparative de la distribution florale dans une portion des Alpes et des Jura,” *Bulletin de la Société Vaudoise des Sciences Naturelles*, vol. 37, pp. 547–579, 1901.
- [32] Graves, A., Fernandez, S., Gomez, F., & Schmidhuber, J. (2006). Connectionist temporal classification: Labelling unsegmented sequence data with recurrent neural networks. In *Proceedings of the 23rd international conference on Machine learning* (pp. 369–376).
- [33] Schuhmann, C., Beaumont, R., Vencu, R., Gordon, C., Kaczmarczyk, T., Coombes, T., Schmid, C., & Kiela, D. (2021). *LAIION-400M: Open Dataset of CLIP-Filtered 400 Million Image-Text Pairs*. arXiv preprint arXiv:2111.02114. <https://arxiv.org/abs/2111.02114>